An Adjustable Quasi-Optical Bandpass Filter—Part I: Theory and Design Formulas

ADEL A. M. SALEH, MEMBER, IEEE

Abstract—A quasi-optical bandpass filter suitable for millimeter and submillimeter wavelengths and in the far infrared region is described. It consists of three or more wire-grid polarizers with quarter-wave spacings. The filter has the advantage over conventional quasi-optical filters, e.g., Fabry–Perot filters, that its bandwidth and the shape of its frequency response are adjustable. This is achieved by changing the angular orientations of the wires of the different polarizers. The filter requires the input electric field to be linearly polarized in a direction perpendicular to the wires of the first grid. The theory of operation is presented and design formulas for the filter are given, under the assumption that ideal wire-grid polarizers are employed. The effects of using realistic grids on the performance of the filter are dealt with in another paper.

I. INTRODUCTION

At MILLIMETER and submillimeter wavelengths and in the far infrared region, low loss and high power handling capability are obtained by performing filtering operations in a quasi-optical form rather than inside a waveguide. The simplest and most commonly used type of quasi-optical filter is a Fabry–Perot resonator employing two or more metallic wire grids [1]–[9]. In such a filter there is no simple provisions for adjusting the bandwidth or the shape of the frequency response. Thus, to obtain some desired response, grids with precise dimensions have to be employed. This makes it difficult to build such filters.

An adjustable quasi-optical bandpass filter which eliminates the above problem is described in this paper. It consists of three or more wire-grid polarizers whose planes are parallel and are spaced at quarter-wave intervals. The bandwidth and shape of the frequency response of the filter can be adjusted without affecting the center frequency by changing the angular orientations of the wires of the different polarizers. The principle of operation of this filter bears some resemblance to that of DeLoach's step-twist-junction waveguide filter [10], [11].

A four-grid filter is shown in Fig. 1 together with a simplified representation which will be employed throughout the paper. In this figure, $x_a, x_b, \cdots$ are in the directions of the wires of grids $a, b, \cdots$, respectively. The θ's are the angles between wires of adjacent grids and the ϕ's are the electrical lengths of the spacings between them ($\phi = 2\pi s/\lambda$, where s is the spacing and λ the operating wavelength). Note that the incident wave is linearly polarized in a direction perpendicular to the wires of the first grid and the transmitted wave is linearly polarized in a direction perpendicular to the wires of the last grid.

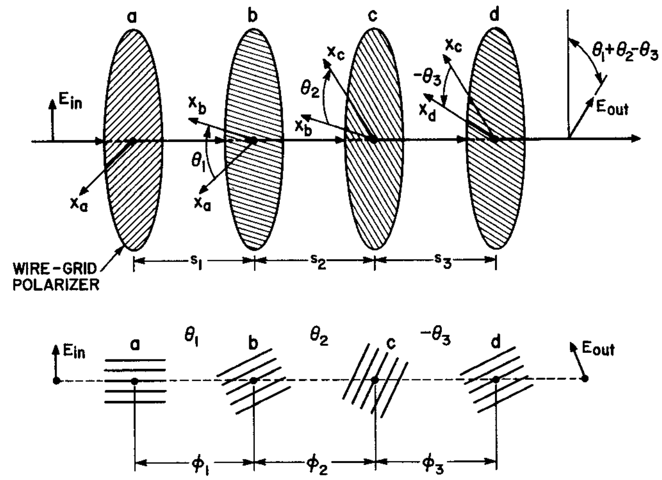

Fig. 1. A four-grid filter and its simplified representation.

The grids will be assumed to be ideal polarizers. That is to say, a wave incident on a grid will be totally reflected or totally transmitted depending, respectively, on whether the electric field vector is parallel or perpendicular to the wires of the grid. This can only be achieved if the grids consist of parallel wires of infinitesimal thickness and spacing. The effects of using realistic grids with finite dimensions are considered in a companion paper [12].

The filter discussed here may superficially appear to be similar to the optical birefringent bandpass filters of the Lyot and the Solc types [13]. However, the operation of these optical filters rests in fact on quite different principles. They employ anisotropic materials and absorption-type polarizers. These polarizers absorb almost all the power at frequencies outside the passband of the filter and partially absorb the power at frequencies within the passband. This makes such filters generally unsuitable for usual communication applications.

II. THE BASIC SECTION OF THE FILTER

The response of a multigrid filter can be calculated conveniently by dividing the filter into basic sections and using matrix cascading formulas. The calculations are greatly simplified by considering a *basic section* to consist of two successive grids together with the space between them. Even though the electric field between the two grids

Manuscript received November 19, 1973; revised February 25, 1974. Part of this work was presented by the author as a post-deadline paper at the 1973 IEEE G-MTT International Microwave Symposium, Boulder, Colo., June 4–6, 1973.
The author is with Bell Laboratories, Crawford Hill Laboratory, Box 400, Holmdel, N. J. 07733.

has two components of polarization, only one component of polarization at each grid (namely, that perpendicular to the wires of the grid) is transmitted. Thus the basic section acts as a two-port network and 2×2 cascading matrices can be used in the analysis. This is true only because the grids are assumed to be ideal polarizers. If this is not the case, more complicated analysis involving 4×4 matrices [12], [14] has to be employed.

To illustrate how a multigrid filter can be subdivided into a number of basic sections, consider the four-grid filter in Fig. 1. One can conceptually slice each of the intermediate grids b and c into grids b',b'' and c',c'', respectively, as shown in Fig. 2. Each of the three sections $a - b'$, $b'' - c'$, and $c'' - d$ is a basic section as defined above. In general an n-section filter has $n + 1$ grids.

A basic section is defined by the angle θ between the wires of the two grids forming the section and the electrical length ϕ of the spacing between them at a given frequency. Let a wave with an electric field E_i perpendicular to the wires of the first grid be at normal incidence on a basic section as shown in Fig. 3. The wave will be unaffected until it reaches the second grid. There, the component of electric field perpendicular to the wires ($E_i \cos\theta$) will be transmitted while that parallel to them ($E_i \sin\theta$) will be reflected towards the first grid. The same kind of partial transmission and reflection will take place at the first grid, then at the second grid, and so on. The end result of these successive reflections is that a wave with an electric field E_r perpendicular to the wires of the first grid, i.e., parallel to E_i, will be reflected by the two-grid structure, and a wave with an electric field E_t perpendicular to the wires of the second grid will be transmitted through it. By adding the fields of the successive passes and summing the resulting infinite series, one obtains the overall field transmission coefficient t and reflection coefficient r for the basic section as

$$t \equiv E_t/E_i = j2 \sin\phi \cos\theta/[\exp(j2\phi) - \cos^2\theta] \quad (1)$$

$$r \equiv E_r/E_i = -\sin^2\theta/[\exp(j2\phi) - \cos^2\theta]. \quad (2)$$

These equations can also be deduced from the work of Groves [15].

From (1) and (2) one observes the following. 1) Changing the sign of θ does not affect t or r. 2) The peak value of $|t|$ as a function of frequency is obtained when ϕ is an odd multiple of $\pi/2$, i.e., when the spacing between the grids is an odd multiple of $\lambda/4$. 3) This peak value of $|t|$ never reaches unity except in the trivial case when $\theta = 0$. Thus a basic section by itself is not suitable as a bandpass filter. 4) When ϕ is a multiple of π, i.e., when the spacing between the grids is a multiple of $\lambda/2$, one obtains $|t| = 0$ and $|r| = 1$. Thus the basic section can be used as a band-reject filter. This fact was recently observed by Hill and Cornbleet [14].

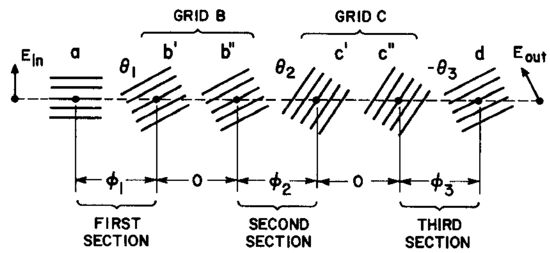

Fig. 2. Subdividing the four-grid filter of Fig. 1 into three basic sections.

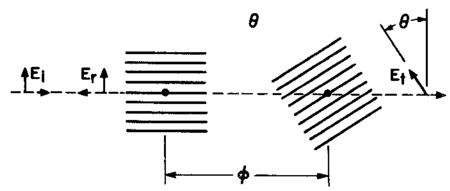

Fig. 3. Basic section of the filter.

The chain or $ABCD$ matrix parameters of a basic section can be shown from (1) and (2) to be

$$A = D = \cos\phi/\cos\theta \quad (3a)$$

$$B = j \sin\phi/\cos\theta \quad (3b)$$

$$C = j(\cos^2\theta - \cos^2\phi)/(\sin\phi \cos\theta). \quad (3c)$$

The field transmission coefficient t_n of a cascade of n sections is obtained by multiplying together the chain matrices of all the sections to obtain the overall chain matrix parameters A_n, B_n, C_n, and D_n, and using the formula

$$t_n = 2/(A_n + B_n + C_n + D_n). \quad (4)$$

III. THE IDEAL TWO-SECTION FILTER

While one basic section by itself does not give 100-percent transmission at any frequency, a cascade of two or more sections can be designed to give 100-percent transmission at any desired frequency. Here we discuss the two-section (i.e., three-grid) filter. Filters with more than two sections are discussed later.

It can be shown from (3) and (4) that a two-section filter can give 100-percent transmission at any desired frequency if both the sections are identical. Two possible realizations of such a symmetric filter are shown in Fig. 4(a) and (b). They correspond, respectively, to the cases where $\theta_1 = \theta_2 = \theta$ and $\theta_1 = -\theta_2 = \theta$. These two realizations have the same response because the characteristics of the basic section do not depend on the sign of θ. The transmission coefficient of either filter is found from (3) and (4) to be

$$t_2 = \frac{\sin\phi \cos^2\theta}{(2\cos^2\phi - \cos^2\theta)\sin\phi + j(1 - 2\cos^2\phi + \cos^2\theta)\cos\phi} \quad (5a)$$

which gives

$$|t_2|^2 = [1 + \tan^4\theta \cot^2\phi]^{-1}. \quad (5b)$$

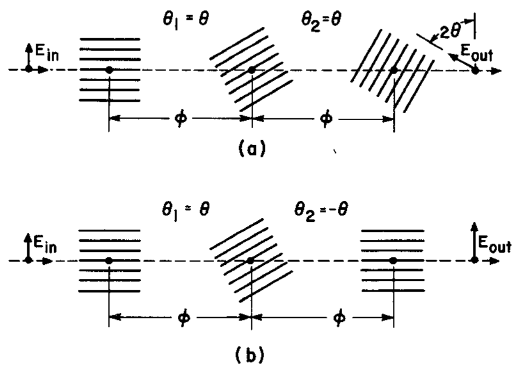

Fig. 4. Two realizations of a symmetric two-section filter.

The subscript 2 in t_2 refers to the number of sections.

It is clear from (5) that, for any value of θ, 100-percent transmission is obtained at $\phi = (2m - 1)\pi/2$, i.e., when the distance between adjacent grids is $(2m - 1)\lambda/4$, where m is a positive integer. Thus transmission resonances occur at $f_m = (2m - 1)f_0$; f_0 being the frequency at which $\phi = \pi/2$. If B is defined as the 3-dB bandwidth at the mth resonance, (5b) gives the 3-dB relative bandwidth:

$$w_m \equiv B/f_m = \frac{4 \tan^{-1}(\cot^2 \theta)}{(2m - 1)\pi}, \qquad m = 1,2,\cdots. \quad (6)$$

Thus the closer θ is to 90°, the narrower is the bandwidth of the filter. A family of curves for $|t_2|^2$, in decibels, as a function of the normalized frequency f/f_0 is shown in Fig. 5 for the first resonance ($m = 1$).

Since the variation of the angle θ changes the bandwidth but leaves the center frequency unchanged, the filter can be called "an adjustable bandwidth filter." The realization of the filter shown in Fig. 4(b) is to be preferred to that in Fig. 4(a) for two reasons. 1) The bandwidth adjustment is achieved by rotating the middle grid alone. 2) The input and output polarizations remain parallel.

The realization shown in Fig. 4(a) is useful as a polarization rotator at frequencies near f_0. This has previously been investigated by Burtner [16], Chu [17], and Hill and Cornbleet [14].

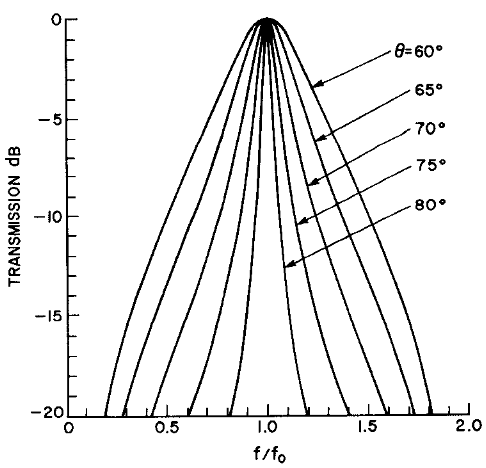

Fig. 5. Frequency response of a two-section filter.

It is worth noting that $\theta_1 = \pm\theta_2$ is a necessary and sufficient condition for obtaining 100-percent transmission through a two-section filter at any given frequency. The equality of ϕ_1 and ϕ_2, however, is not necessary for that purpose. If $\phi \equiv (\phi_1 + \phi_2)/2$, then just as in the symmetric case, $|t_2| = 1$ at $\phi = (2m - 1)\pi/2$. In addition, if $\phi_1 \neq \phi_2$, then $|t_2| = 1$ at $\phi = m\pi$. However, if $\phi_1 = \phi_2 = \phi$, then $|t_2| = 0$ at $\phi = m\pi$ as can be deduced from (5). Hence, the existence of the null in $|t_2|$ at $\phi = m\pi$ depends critically on the equality of ϕ_1 and ϕ_2. Thus if such a structure is to be used as a band-reject filter as was suggested by Hill and Cornbleet [14], then a high degree of tolerance has to be maintained in spacing the grids. This is not the case when the structure is used as a bandpass filter.

IV. IDEAL MULTISECTION FILTERS

The two-section filter is essentially a single-pole filter. To obtain a frequency response with a sharper edge, multisection filters are required.

Using (3) and (4), it can be shown that the transmission coefficient of a cascade of n identical sections ($n + 1$ grids) is given, for $n \geq 1$, by

$$t_n = \left\{T_n\left[\frac{\cos\phi}{\cos\theta}\right] + j\,\frac{2\sin^2\phi - \sin^2\theta}{2\sin\phi\cos\theta}\,U_{n-1}\left[\frac{\cos\phi}{\cos\theta}\right]\right\}^{-1} \quad (7a)$$

which gives

$$|t_n|^2 = \left\{1 + \left(\frac{\sin^2\theta}{2\sin\phi\cos\theta}\,U_{n-1}\left[\frac{\cos\phi}{\cos\theta}\right]\right)^2\right\}^{-1}. \quad (7b)$$

In the above equations, T_n and U_n denote Chebyshev polynomials of the first and second kind, respectively. They are defined by

$$T_n(\cos\psi) \equiv \cos(n\psi) \quad (8)$$

$$U_n(\cos\psi) \equiv \frac{\sin[(n + 1)\psi]}{\sin\psi}. \quad (9)$$

A careful examination of (7b) leads to the following observations. 1) Just as in the case of a two-section filter, the bandwidth of a multisection filter decreases as θ increases towards 90°; however, at the same time, the level of the ripples in the passband increases considerably. 2) For $n \geq 5$, the filter does not have an equal-ripple (ER) response (for $n = 3$ or 4, an ER response is obtained by virtue of symmetry).

The above observations indicate that a cascade of more than two identical sections is generally not suitable as a bandpass filter. However, as will be shown below, bandpass filters with any desired characteristic, e.g., with maximally flat (MF) or ER response, can be built provided that nonidentical sections are employed.

To obtain a frequency response which is symmetric with respect to the center frequency, we will restrict ourselves to the case where the electric lengths (the ϕ's) of all the sections are identical. Furthermore, in order that the transmission coefficient reaches unity at least once within the passband, we restrict ourselves to electrically symmetric multisection filters (this is a sufficient but not a necessary condition for this purpose). Thus for an n-section filter with $n = 2,3,4,5,\cdots$, the angles between the wires of the successive sections will be respectively, $\theta_1\theta_1$, $\theta_1\theta_2\theta_1$, $\theta_1\theta_2\theta_2\theta_1$, $\theta_1\theta_2\theta_3\theta_2\theta_1,\cdots$, etc. In general there are $[(n+1)/2]$ different θ's in a symmetric n-section filter (the square brackets indicate "the integer part of"). As before, the sign of each of the θ's is arbitrary. Several symmetric multisection filters are shown in Fig. 6. It is noted that for even values of n, the input and output polarizations can be made parallel. This is not the case in general for odd values of n.

Using (3) and (4), one obtains, after some algebraic manipulations, the power transmission coefficient for a symmetric n-section filter as

$$|t_n|^2 = \frac{\sin^2\phi}{\sin^2\phi + \left[2^{n-2}\sin^2\theta_1 F_n(\phi,\boldsymbol{\theta}) / \prod_{k=1}^{n}\cos\theta_k\right]^2} \tag{10}$$

where $\boldsymbol{\theta} = \{\theta_1,\theta_2,\cdots,\theta_{[(n+1)/2]}\}$, $\theta_k \equiv \theta_{n+1-k}$ for $k > [(n+1)/2]$, and $F_n(\phi,\boldsymbol{\theta})$ is given in Table I for $n = 1$ to 6.

The design of MF and ER filters based on the result given in (10) is discussed in the next two sections.

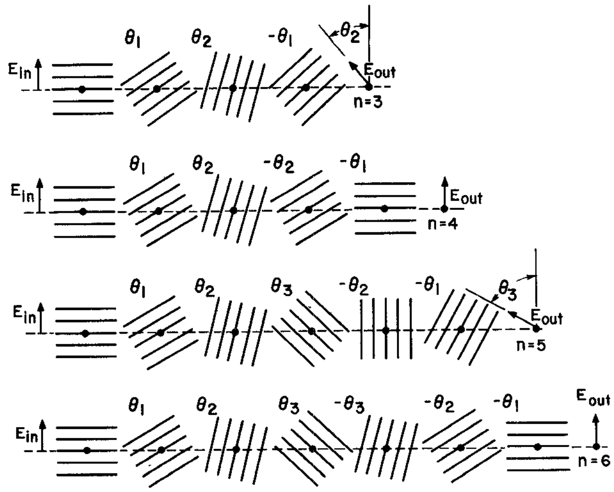

Fig. 6. Symmetric multisection filters.

TABLE I
VALUES OF $F_n(\phi, \boldsymbol{\theta})$ FOR (10)

n	$F_n(\phi,\boldsymbol{\theta})$
1	1
2	$\cos\phi$
3	$\cos^2\phi-(C_2-C_1^2)/(4\sin^2\theta_1)$
4	$\cos\phi[\cos^2\phi-(2C_2-C_1C_2-C_1^2)/(4\sin^2\theta_1)]$
5	$\cos^4\phi+p\cos^2\phi+q$ $p=[C_1(C_1+C_2+C_3)-2C_2-C_3]/(4\sin^2\theta_1)$ $q=(C_2^2-C_1^2C_3)/(16\sin^2\theta_1)$
6	$\cos\phi[\cos^4\phi+r\cos^2\phi+s]$ $r=[C_1(C_1+C_2+2C_3)-2C_2-2C_3]/(4\sin^2\theta_1)$ $s=[C_2(C_2+2C_3-C_1C_3)-2C_3C_1^2]/(16\sin^2\theta_1)$

Note: $C_k \equiv \cos^2\theta_k$ throughout the table.

V. DESIGN OF MF AND ER FILTERS

Consider a symmetric multisection filter. Let f_0 be the frequency at which $\phi = \pi/2$, i.e., the spacing between adjacent grids $s = \lambda_0/4$. Transmission resonances occur at $f_m = (2m-1)f_0$, $m = 1,2,\cdots$. For a filter with bandwidth B operating at the mth resonance, the relative bandwidth is given by

$$w_m \equiv B/f_m = w/(2m-1) \tag{11a}$$

where

$$w \equiv B/f_0. \tag{11b}$$

The design procedure will be based on w rather than on w_m. Of course, $w = w_m$ if one is operating at the first resonance ($m = 1$).

To design an MF or ER filter, besides w, one needs to know the maximum attenuation allowed in the passband; let this quantity be α decibels. This corresponds to a minimum power transmission coefficient τ related to α by

$$\alpha = -10\log_{10}\tau. \tag{12}$$

Let us now define

$$\Delta \equiv \pi w/4 \tag{13}$$

$$\rho \equiv [\tau/(1-\tau)]^{1/2}. \tag{14}$$

A look at (10) reveals that the manner by which the quantity $F_n(\phi,\boldsymbol{\theta})/\sin\phi$ varies with ϕ, i.e., with frequency, indicates the type of response of the filter. The function $F_n(\phi,\boldsymbol{\theta})$ is shown from Table I to be a polynomial in $\cos\phi$. If all the coefficients of this polynomial, with the exception of the coefficient of the highest power of $\cos\phi$, are set to zero, the filter will have an MF response. On the other hand, if these coefficients are chosen such that $F_n(\phi,\boldsymbol{\theta})/\sin\phi$ has equal ripples the filter will have an ER response. With this in mind, the values of the θ's for symmetric multisection filters can be calculated to obtain MF or ER response with given values of Δ and ρ. The results are given below for two-, three-, and four-section filters.

Two-Section Filter:

$$\cot^2\theta_1 = \rho\tan\Delta. \tag{15}$$

MF Three-Section Filter:

$$x = [\rho\sin^2(\Delta/2)\cos\Delta]^{1/2} \tag{16a}$$

$$\cos^2\theta_1 = 2x[(x^2+1)^{1/2} - x] \tag{16b}$$

$$\cos\theta_2 = \cos^2\theta_1. \quad (16c)$$

ER Three-Section Filter:

$$x = \{\tfrac{1}{2}[(1+\rho^2)^{1/2} - 1][1-\cos\Delta]\}^{1/2} \quad (17a)$$

$$\cos^2\theta_1 = 2x[(x^2+1)^{1/2} - x] \quad (17b)$$

$$\cos\theta_2 = \cos^2\theta_1\rho/[(1+\rho^2)^{1/2} - 1]. \quad (17c)$$

MF Four-Section Filter:

$$x = 4\rho\sin^3\Delta/\cos\Delta \quad (18a)$$

$$\cos^6\theta_1 - x\cos^4\theta_1 + 3x\cos^2\theta_1 - 2x = 0 \quad (18b)$$

$$\cos^2\theta_2 = \cos^4\theta_1/(2-\cos^2\theta_1). \quad (18c)$$

ER Four-Section Filter:

$$x = 2\rho\sin\Delta(1-\cos\Delta) \quad (19a)$$

$$y = 2(1-\cos\Delta)(2+\cos\Delta) \quad (19b)$$

$$\cos^6\theta_1 - (x+y)\cos^4\theta_1 + (3x+y)\cos^2\theta_1 - 2x = 0 \quad (19c)$$

$$\cos^2\theta_2 = x\tan^2\theta_1. \quad (19d)$$

The frequency responses of a two-section filter, a MF four-section filter, and an ER four-section filter are shown in Fig. 7 for comparison. Each of the filters has a maximum passband attenuation $\alpha = 1$ dB and a relative bandwidth $w = 0.05$. The angles indicated in the figure were calculated using the above equations and the responses were plotted from (10).

For filters with more than four sections, an exact analysis becomes quite involved. However, since the desired relative bandwidth w is usually a small quantity, approximate solutions with $w \ll 1$ are useful. This is done in the next section.

VI. APPROXIMATE DESIGN OF NARROW-BAND FILTERS

With $w \ll 1$, the equations for the θ's obtained in the previous section can be approximated by simple expressions. In fact, by noticing an analog between our n-section filter and homogeneous $(n-1)$-section stepped-impedance quarter-wave transformers [18, ch. 6], the approximate solutions can be extended to any value of n greater than one. The analog is obtained by replacing n, w, $(\pi/2) - \theta_1$, $(\pi/2) - \theta_k$, and α in our case, respectively, by $n-1$, w_q, $(2/V_1)^{1/2}$, $2/(V_k)^{1/2}$, and L_{Ar} in [18, ch. 6]. The results are given below in terms of w and ρ which are defined in (11)–(14) and the quantities

$$a_1 \equiv \left[\sin\left(\frac{\pi}{2(n-1)}\right)\right]^{-1} \quad (20a)$$

$$a_k \equiv \left[\sin\left(\frac{2k-1}{2(n-1)}\pi\right)\sin\left(\frac{2k-3}{2(n-1)}\pi\right)\right]^{-1/2}, \quad k = 2,3,\cdots,[(n+1)/2]. \quad (20b)$$

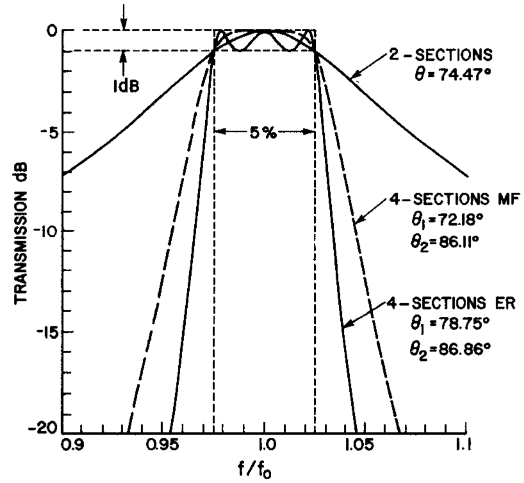

Fig. 7. Comparison of the frequency responses of a two-section filter, an MF four-section filter, and an ER four-section filter ($\alpha = 1$ dB, $w = 0.05$).

MF n-Section Filters:

$$g \equiv \rho^{1/(n-1)} \quad (21a)$$

$$\theta_1 \simeq \frac{\pi}{2} - \left[\frac{\pi}{4}wa_1g\right]^{1/2} \quad (21b)$$

$$\theta_k \simeq \frac{\pi}{2} - \frac{\pi}{4}wa_kg, \qquad k = 2,3,\cdots,[(n+1)/2]. \quad (21c)$$

ER n-Section Filters:

$$h \equiv \sinh\left[\frac{1}{n-1}\sinh^{-1}(\rho)\right] = \tfrac{1}{2}[(1+\rho^2)^{1/2}+\rho]^{1/(n-1)} - \tfrac{1}{2}[(1+\rho^2)^{1/2}+\rho]^{-1/(n-1)} \quad (22a)$$

$$\theta_1 \simeq \frac{\pi}{2} - \left[\frac{\pi}{4}wa_1h\right]^{1/2} \quad (22b)$$

$$\theta_k = \frac{\pi}{2} - \frac{\pi}{4}w[1 + a_k^2(a_1^{-2}+h^2)]^{1/2}, \quad k = 2,3,\cdots,[(n+1)/2]. \quad (22c)$$

From (20)–(22), one obtains for both MF and ER filters

$$\theta_1 \simeq 90 - b_1w^{1/2} \text{ degrees} \quad (23a)$$

$$\theta_k \simeq 90 - b_kw \text{ degrees}, \quad k = 2,3,\cdots,[(n+1)/2] \quad (23b)$$

where the numerical values of the b_k are given in Table II for various values of the maximum allowable passband attenuation α, for $n = 2$–8 sections.

To demonstrate the accuracy of the above equations, consider a four-section filter with maximum passband attenuation $\alpha = 1.0$ dB and a relative bandwidth at the first resonance $w = 0.05$. For an MF response, (23) gives $\theta_1 \simeq 72.03°$ and $\theta_2 \simeq 86.01°$, while the exact analysis of (18) gives $\theta_1 = 72.18°$ and $\theta_2 = 86.11°$. For an ER

TABLE II
VALUES OF b_k FOR (23)

n	Type	k	Maximum Passband Attenuation dB								
			0.01	0.02	0.05	0.10	0.20	0.50	1.00	2.00	3.01
2	-	1	231.7	194.8	154.8	130.0	109.0	85.9	71.2	58.1	50.8
3	MF	1	129.0	118.3	105.4	96.6	88.5	78.5	71.5	64.6	60.4
		2	290.4	244.2	194.0	162.9	136.6	107.7	89.2	72.8	63.6
	ER	1	107.2	97.8	86.3	78.2	70.5	60.6	53.2	45.5	40.7
		2	210.4	178.6	144.7	124.3	107.6	90.4	80.6	73.2	69.9
4	MF	1	119.1	112.4	104.1	98.2	92.6	85.6	80.4	75.1	71.8
		2	175.1	156.0	133.8	119.1	105.9	90.4	79.7	69.6	63.6
	ER	1	90.5	84.4	76.6	70.7	64.8	56.8	50.5	43.6	39.2
		2	115.2	103.8	91.0	82.7	75.7	68.0	63.5	59.9	58.3
5	MF	1	120.0	114.9	108.5	103.8	99.3	93.6	89.3	84.9	82.1
		2	161.7	148.2	132.1	121.1	110.9	98.4	89.6	80.9	75.7
		3	104.1	95.4	85.0	77.9	71.4	63.4	57.7	52.1	48.7
	ER	1	85.1	80.0	73.3	68.2	62.9	55.6	49.6	43.0	38.7
		2	97.3	89.7	80.7	74.8	69.6	63.8	60.2	57.4	56.1
		3	71.5	67.2	62.3	59.2	56.5	53.6	51.8	50.5	49.9
6	MF	1	123.7	119.5	114.2	110.2	106.4	101.5	97.7	93.8	91.3
		2	165.2	154.1	140.6	131.1	122.2	111.1	103.0	95.0	90.0
		3	91.8	85.7	78.1	72.9	67.9	61.7	57.3	52.8	50.0
	ER	1	82.6	78.0	71.9	67.1	62.0	55.0	49.1	42.7	38.4
		2	90.6	84.3	76.8	71.8	67.3	62.1	59.0	56.4	55.3
		3	62.7	60.0	56.8	54.7	52.9	50.9	49.7	48.8	48.4
7	MF	1	128.5	124.9	120.2	116.7	113.4	109.0	105.6	102.1	99.8
		2	174.5	164.7	152.5	143.9	135.7	125.3	117.7	110.0	105.2
		3	90.3	85.2	79.0	74.5	70.2	64.9	60.9	56.9	54.5
		4	77.3	72.9	67.6	63.7	60.1	55.5	52.1	48.7	46.6
	ER	1	81.2	76.9	71.1	66.4	61.6	54.7	48.9	42.5	38.3
		2	87.3	81.7	74.9	70.3	66.1	61.3	58.4	56.0	54.8
		3	59.4	57.2	54.6	53.0	51.5	49.9	48.9	48.2	47.8
		4	55.9	54.2	52.2	51.0	49.8	48.6	47.9	47.3	47.1
8	MF	1	133.7	130.4	126.2	123.1	120.1	116.0	113.0	109.7	107.6
		2	186.4	177.4	166.1	158.0	150.3	140.4	133.1	125.5	120.8
		3	92.6	88.2	82.6	78.5	74.7	69.8	66.1	62.4	60.0
		4	73.2	69.6	65.2	62.0	59.0	55.1	52.2	49.3	47.4
	ER	1	80.4	76.3	70.6	66.1	61.3	54.5	48.8	42.4	38.2
		2	85.4	80.2	73.8	69.4	65.4	60.9	58.0	55.7	54.6
		3	57.7	55.8	53.6	52.1	50.8	49.4	48.5	47.9	47.5
		4	53.3	52.0	50.5	49.6	48.7	47.8	47.2	46.8	46.6

response, (23) gives $\theta_1 \simeq 78.71°$ and $\theta_2 \simeq 86.83°$, while the exact analysis of (19) gives $\theta_1 = 78.75°$ and $\theta_2 = 86.86°$. The accuracy of (23) holds reasonably well even for w as high as 0.2.

The number of sections needed for some application is determined from the required steepness of the frequency-response curve beyond the edge of the passband. Let the normalized frequency be defined as

$$\delta = 2(f - f_0)/f_0 \qquad (24)$$

where f_0 is the center frequency at the first resonance. It can be shown that in the vicinity of the passband, i.e., $\delta \ll 1$, and for $w \ll 1$, (10) is approximated by

$$|t_n|^2 \simeq \{1 + [\rho^{-1}(\delta/w)^{n-1}]^2\}^{-1} \qquad (25)$$

for MF filters, and

$$|t_n|^2 \simeq \{1 + [\rho^{-1}T_{n-1}(\delta/w)]^2\}^{-1} \qquad (26)$$

for ER filters, where T_n is the Chebyshev polynomial of the first kind defined in (8). The above equations show that an n-section filter has $n - 1$ poles. The equations are identical to those of standard MF and ER filters which are found in many filter textbooks such as [18, sec. 4.03] (in this reference, δ/w is replaced by ω'/ω_1'). Given the type of filter, i.e., MF or ER, the number of sections and the allowable passband attenuation, one can use (25) or (26) to calculate δ/w for any attenuation level beyond the passband edge. The results are plotted in [18] and will not be repeated here. As an example, [18, fig. 4.03-8] shows that the response of a three-pole (four-section) ER filter with 1-dB passband ripples has a 25-dB bandwidth which is 2.18 times greater than the filter's nominal bandwidth; this number becomes 1.19 for the corresponding seven-pole (eight-section) filter.

VII. CONCLUSIONS

The quasi-optical bandpass filter presented in this paper has potential applications at millimeter and submillimeter wavelengths and in the far infrared region. It has the advantage over conventional quasi-optical filters, e.g., those of the Fabry–Perot type, that its bandwidth and shape of its frequency response curve are adjustable. The filter requires the input wave to be linearly polarized. Thus it is not suitable for use with incoming waves having circular polarization or linear polarization of an unknown direction.

This filter can be used in conjunction with waveguide systems. This is particularly attractive if the powers involved are so high that overheating or arcing would take place in conventional waveguide filters. For this purpose, one needs an efficient waveguide-to-beam launcher such as a hybrid or a dual mode horn used in conjunction with a lens or a parabolic reflector [19].

Throughout this paper, the wave was assumed to be at normal incidence on the filter. It is possible to modify the design formulas to include oblique incidence. Having the wave at oblique incidence causes the reflected wave to be separated from the incident wave which is necessary if the filter is to be used as a diplexer. In this case, some loss caused by the shifting of the beam as it bounces back and forth between the grids needs to be taken into account. This loss is similar to the walk-off loss occurring in conventional Fabry–Perot diplexers [20].

ACKNOWLEDGMENT

The author wishes to thank A. B. Crawford, T. S. Chu, and J. A. Arnaud for stimulating discussions.

REFERENCES

[1] E. A. Lewis and J. P. Casey, "Metal grid interference filter," *J. Opt. Soc. Amer.*, vol. 41, p. 360, May 1951.
[2] W. Culshaw, "Reflectors for a microwave Fabry-Perot interferometer," *IRE Trans. Microwave Theory Tech.*, vol. MTT-7, pp. 221–228, Apr. 1959.
[3] ——, "High resolution millimeter wave Fabry-Perot interferometer," *IRE Trans. Microwave Theory Tech.*, vol. MTT-8, pp. 182–189, Mar. 1960.
[4] K. F. Renk and L. Genzel, "Interference filters and Fabry-Perot interferometers for the far infrared," *Appl. Opt.*, vol. 1, pp. 643–648, Sept. 1962.
[5] R. Ulrich, K. F. Renk, and L. Genzel, "Tunable submillimeter interferometers of the Fabry-Perot type," *IEEE Trans. Microwave Theory Tech.*, vol. MTT-11, pp. 363–371, Sept. 1963.
[6] R. Ulrich, "Interference filters for the far infrared," *Appl. Opt.*, vol. 7, pp. 1987–1996, Oct. 1968.
[7] R. J. Bell, H. V. Romero, and J. M. Blea, "Theory and experiments for multielement grid filters in a dielectric," *Appl. Opt.*, vol. 9, pp. 2350–2358, Oct. 1970.

[8] M. M. Pradhan, "Multigrid interference filters for the far infrared region," *Infrared Phys.*, vol. 11, pp. 241–245, Dec. 1971.
[9] M. M. Pradhan, X. Gerbaux, and A. Hadni, "Narrow band metallic grid filters for the very far infrared," *Infrared Phys.*, vol. 12, pp. 263–266, Oct. 1972.
[10] B. C. DeLoach, Jr., "Step-twist-junction waveguide filters," *IRE Trans. Microwave Theory Tech.*, vol. MTT-9, pp. 130–135, Mar. 1961.
[11] ——, "Direct-, and quarter-wave-coupled microwave bandpass filters with adjustable transmission characteristics and fixed center frequencies," *IEEE Trans. Microwave Theory Tech.* (*1963 Symposium Issue*), vol. MTT-12, pp. 73–77, Jan. 1964.
[12] A. A. M. Saleh, "An adjustable quasi-optical bandpass filter—Part II: Practical considerations," this issue, pp. 734–739.
[13] E. O. Ammann, "Synthesis of optical birefringent networks," in *Progress in Optics*, E. Wolf, Ed. Amsterdam, The Netherlands: North Holland, 1971, ch. IV, pp. 123–177.
[14] N. Hill and S. Cornbleet, "Microwave transmission through a series of inclined gratings," *Proc. Inst. Elec. Eng.*, vol. 120, pp. 407–412, Apr. 1973.
[15] W. E. Groves, "Transmission of electromagnetic waves through pairs of parallel wire grids," *J. Appl. Phys.*, vol. 24, pp. 845–854, July 1953.
[16] R. L. Burtner, U. S. Patent 2 544 936, May 29, 1951.
[17] T. S. Chu, unpublished work, 1971.
[18] G. L. Matthaei, L. Young, and E. M. T. Jones, *Microwave Filters, Impedance-Matching Networks, and Coupling Structures.* New York: McGraw-Hill, 1964.
[19] R. J. Chaffin and J. B. Beyer, "A low-loss launcher for the beam waveguide," *IEEE Trans. Microwave Theory Tech.* (Corresp.), vol. MTT-12, p. 555, Sept. 1964.
[20] J. A. Arnaud, A. A. M. Saleh, and J. T. Ruscio, "Walk-off effects in Fabry–Perot diplexers," vol. MTT-22, pp. 486–493, May 1974.

An Adjustable Quasi-Optical Bandpass Filter—Part II: Practical Considerations

ADEL A. M. SALEH, MEMBER, IEEE

Abstract—**This paper investigates the effects of using realistic grids on the performance of the adjustable quasi-optical bandpass filter presented in Part I. The theory given here is in excellent agreement with measurements performed on a three-grid filter in the 50–75-GHz band.**

I. INTRODUCTION

IN PART I of this paper [1], an adjustable quasi-optical bandpass filter was described. The theory of operation and the design formulas reported were developed under the assumption that the wire-grid polarizers employed were ideal. To be more specific, let the field reflection and transmission coefficients for a plane wave at normal incidence on a parallel-wire grid be denoted, respectively, by $r_{||}$ and $t_{||}$ when the electric field is parallel to the wires, and $r_\perp$ and $t_\perp$ when it is perpendicular to the wires. In Part I of this paper it was assumed that $r_{||} = -1$, $t_{||} = 0$, $r_\perp = 0$, and $t_\perp = 1$. This would require the wires of the grids to have infinitesimal thickness and spacing. Thus in practice, such values of the r's and t's can only be achieved approximately. In this paper, the effects of using realistic grids on the performance of the filter are investigated.

II. WIRE-GRID POLARIZERS

In this section, the values of $r_{||}$, $t_{||}$, $r_\perp$, and $t_\perp$ are given for two common types of grids. The grids will be assumed to be lossless, i.e.,

$$|r_{||}|^2 + |t_{||}|^2 = 1$$
$$|r_\perp|^2 + |t_\perp|^2 = 1 \tag{1}$$

and to have a thickness small compared to a wavelength, i.e.,

$$t_{||} = 1 + r_{||} \qquad t_\perp = 1 + r_\perp. \tag{2}$$

From (1) and (2), and from the fact that the grids are inductive for the parallel polarization and capacitive for the perpendicular polarization, the r's and t's can be written as functions of two positive real parameters $\psi_{||}$ and $\psi_\perp$ in the forms

$$r_{||} = -\cos\psi_{||} \exp(-j\psi_{||}) \tag{3}$$
$$t_{||} = j \sin\psi_{||} \exp(-j\psi_{||}) \tag{4}$$
$$r_\perp = -j \sin\psi_\perp \exp(-j\psi_\perp) \tag{5}$$
$$t_\perp = \cos\psi_\perp \exp(-j\psi_\perp). \tag{6}$$

The grids of interest for the filter are those which act as reasonably good polarizers, i.e., $|r_{||}|$, $|t_\perp| \simeq 1$ and $|t_{||}|$, $|r_\perp| \ll 1$. Thus the quality of a grid will be described by the two coefficients $|t_{||}|$ and $|r_\perp|$. The smaller these coefficients are, the better is the grid. Clearly, since $|t_{||}| = \sin\psi_{||}$ and $|r_\perp| = \sin\psi_\perp$, the magnitude and phase of any of the coefficients given in (3)–(6) can be calculated from $|t_{||}|$ and $|r_\perp|$. It is emphasized that this is only true since the grids are assumed to be lossless and thin in comparison to the wavelength.

Two common types of grids are shown in Fig. 1. The first grid, Fig. 1(a), consists of thin metallic strips of

Manuscript received November 19, 1973; revised February 25, 1974.
The author is with Bell Laboratories, Crawford Hill Laboratory, Box 400, Holmdel, N. J. 07733.